# Crystalline and Supermolecular Structure of Polylactide in Relation to the Crystallization Method

**Mirosław Pluta, Andrzej Galeski**

*Centre of Molecular and Macromolecular Studies, Polish Academy of Sciences, Sienkiewicza 112, 90-363 Łódź, Poland*

Received 25 April 2001; accepted 7 February 2002

**ABSTRACT:** The effect of thermal treatment on the crystalline and supermolecular structure of polylactide was investigated. The samples were isothermally crystallized by two methods, the crystallization temperature being reached (1) via cooling from the melt and (2) via heating from the glassy, amorphous state. The samples were crystallized over a broad temperature range of 70–130°C. The glassy state was produced by the quenching of the polymer melt to ambient temperature. The morphology and structural features of the samples were examined with X-ray techniques (wide-angle and small-angle X-ray scattering), small-angle light scattering, polarizing light microscopy, and differential scanning calorimetry. The results showed similar structures on the lamellar level for samples prepared by the two methods under similar time and temperature conditions. Crystal perfection increased with the crystallization temperature. This was accompanied by an evolution of the spherulitic structure: the spherulites were larger in samples crystallized via cooling from the melt than those in samples crystallized via heating from the glassy, amorphous state. The thermal properties were influenced markedly by the initial crystallinity of the polymer, but differentiation of the supermolecular structures between samples crystallized according to the two protocols did not affect their thermal behavior. The structure of each sample was correlated with its viscoelastic properties. The viscoelastic response was sensitive to the crystallinity level but depended less on the sizes of the spherulites.
 J Appl Polym Sci 86: 1386–1395, 2002

**Key words:** polylactide; morphology; thermal properties; viscoelastic properties

## INTRODUCTION

Interest in polylactides (PLAs) has grown rapidly in recent years because they exhibit promising physical properties; are processable with standard plastic processing equipment, including extrusion, molding, blown film, and foaming operations; and can be made from annually renewable resources. In particular, the degradation of PLAs by hydrolysis in the environment into harmless, natural products in a short time period, from about 0.5 to 2 years (conventional plastics such as polystyrene and polyethylene require 500–1000 years to degrade[1]), has received much attention from an ecological viewpoint. Because of their good mechanical properties and appearance, PLAs are considered suitable materials for packaging and consumer goods.[1,2] PLAs also find applications in the field of medicine[3] because, as biocompatible materials, they are metabolized into nontoxic compounds in the body in due course. Their physical properties can easily be modified by changes in their stereochemical structure through the polymerization of a controlled mixture of the L- and D-isomers,[4] by copolymerization,[5] or by blending.[6–8] Stereocomplex blends made from linear L- and D-PLAs[9,10] or from a combination of linear and star-shaped PLAs or two star-shaped PLAs[11,12] constitute a new class of materials with interesting and modified physical properties exceeding the respective properties of the homopolymers used.

The goal of this work was PLA with slightly disturbed stereoregularity through the incorporation of a small amount of D-lactide into L-isomer. The research was primarily focused on the determination of the influence of the thermal history of samples before crystallization on the crystalline and supermolecular structure. Two types of processed PLA samples were considered, the crystallization temperature being reached (1) via cooling from the melt and (2) via heating from the glassy, amorphous state. A quenched, amorphous sample was obtained by solidification of the melt to ambient temperature. In most other polymers, including polyolefins, a large number of small crystals are formed during quenching, preventing any further significant rearrangement in the amorphous phase and additional crystallization when the sample is heated again to the crystallization temperature. One exception is poly(ethylene terephthalate), which can be quenched effectively to an almost entirely amorphous state and then crystallized when the temperature is increased above the glass temper-

*Correspondence to:* M. Pluta (mpluta@bilbo.cbmm.lodz.pl).
Contract grant sponsor: Polish State Committee for Scientific Research; contract grant number: 7 TO8E 027 19.

Journal of Applied Polymer Science, Vol. 86, 1386–1395 (2002)

ature. The possibility of such an operation for PLA was one of our research goals. Apart from the overall crystallization, primary spherulite nucleation was a concern of ours because quenching usually produces plenty of primary nuclei.

Isothermal crystallization was carried out over a broad range of temperatures above the glass transition. The crystalline structures and morphologies of the samples were investigated with several techniques, including X-ray scattering and diffraction, thermal analysis, light scattering, and light microscopy (LM). Structural investigations were correlated with viscoelastic properties determined with dynamic mechanical thermal analysis (DMTA) within a temperature range covering the glass transition and the $\alpha$-relaxation process.

## EXPERIMENTAL

### Materials

PLA with a weight-average molecular weight of 166,000 and a polydispersity index of 2.0, supplied by Cargill-Dow, Inc. (Minnetonka, MN), was used in this study. This polymer, with mostly an L-configuration, consists of 4.1% D-lactide in the main chain and a residual lactide content of 0.27%.

### Sample preparation

PLA as received was dried at 105°C for 4 h at a reduced pressure before processing. Sheets 1 mm thick were prepared by compression molding at 185°C. The samples were crystallized isothermally, and the crystallization temperature was reached (1) via cooling from the melt and (2) via heating from the glassy, amorphous state. The glassy, amorphous state was achieved by solidification of the molten polymer in air at ambient temperature. The isothermal crystallization temperature of both kinds of samples was set at 70, 80, 90, 100, 110, 120, or 130°C. The crystallization was carried out between a pair of flat and polished aluminum blocks stabilized at a given temperature for 6 h. The samples were then stored in a desiccator at ambient temperature. Isothermally crystallized samples for which the crystallization temperature was reached via cooling from the melt are denoted CT, and those for which the crystallization temperature was reached via heating from the glassy, amorphous state are marked AT, where T refers to the crystallization temperature.

### Measurements

The PLA samples were investigated with several complementary techniques. The thermal behavior was characterized with a TA Instruments 2920 differential scanning calorimeter (New Castle, DE) during heating at a rate of 10°C/min under a nitrogen flow.

The crystalline structure was investigated with a wide-angle X-ray scattering (WAXS) technique. Measurements were performed in reflection geometry at ambient temperature with an automated computer-controlled X-ray diffractometer operating at 30 kV and 30 mA (nickel-filtered Cu K$\alpha$ radiation) within a $2\theta$ range of 10–35° with a step of 0.05°.

Small-angle X-ray scattering (SAXS) was used for the study of the lamellar structure. A PW 1830 generator (Philips Analytical X-Ray B.V., Eindhoven, The Netherlands) operating at 50 kV and 30 mA (nickel-filtered Cu K$\alpha$ radiation) and a Kiessig-type pinhole camera equipped with a collimator system providing point illumination were used. The distance between the sample and the detector was set at 1100 mm, and the exposition time was set at 24 h. The resolution of the camera was up to 80 nm. The two-dimensional SAXS patterns were recorded on imaging plates (Eastman Kodak, Rochester, NY) under vacuum conditions. Exposed imaging plates were read with a PhosphorImager Si scanner (Molecular Dynamics, Sunnyvale, CA).

The supermolecular structure was examined with polarized LM and small-angle light scattering (SALS). These studies were performed on thinner 20-$\mu$m specimens prepared by crystallization at the specified temperatures with a Linkam THMS 600 hot stage (Linkham Scientific Instruments Ltd., Epsom, UK). The specimens were sandwiched between two glass slides. LM (Polish Optical Works, Warsaw) images were recorded with a CCD-4012A television camera (Videotronic, Neumünster, Germany).

The SALS studies were carried out for samples placed between crossed polaroids, with a He–Ne laser used as a light source with a wavelength of $\lambda = 0.6328$ $\mu$m. The scattering patterns were recorded photographically. The light intensity distribution versus the scattering angle determined at the azimuthal angle $\mu = 45°$ was used for calculations of the average spherulite radius ($\langle R \rangle$).[13]

The viscoelastic properties of the PLA samples were measured with an MkIII DMTA apparatus (Rheometric Scientific, Inc., Epsom, UK) in a dual-cantilever bending mode. The dynamic storage modulus ($E'$) and loss factor (tan $\delta$) were measured at a constant frequency of 1 Hz as functions of temperature from 0 to 150°C at a heating rate of 2°C/min. In the lower temperature region, between 0 and −100°C, no discernible relaxation processes in the $E'$ or tan $\delta$ dependencies were found.

## RESULTS AND DISCUSSION

### X-ray results

Figure 1(a,b) shows X-ray diffractograms for selected samples crystallized from the melt (type C) and from

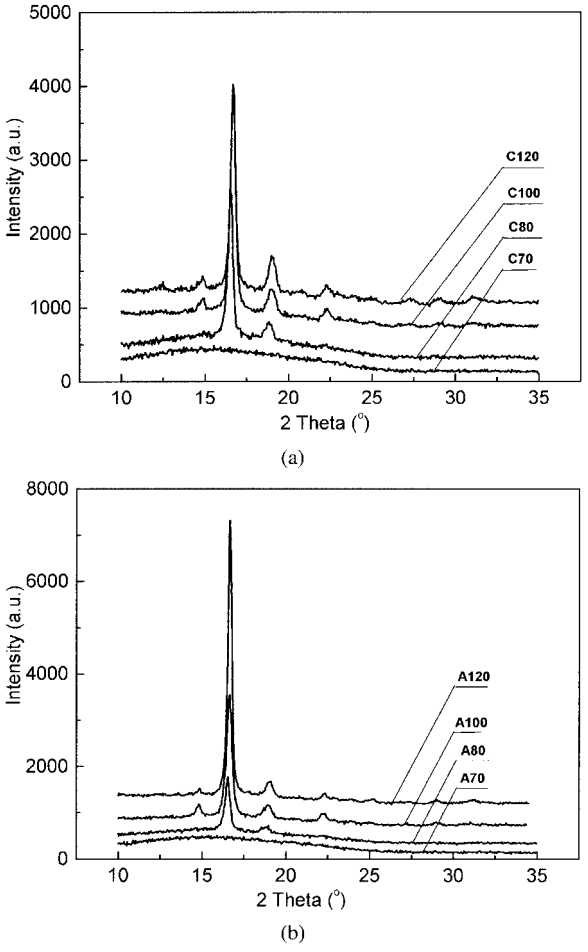


**Figure 1** WAXS 2$\theta$ intensity distributions for PLA samples crystallized isothermally (a) via cooling from the melt and (b) via heating from the quenched, glassy, amorphous state at 70, 80, 100, and 120°C.

the quenched, amorphous state (type A) at the same temperatures: 70, 80, 100, and 120°C. Samples prepared at the lowest temperature, C70 and A70, show a scattered intensity distribution with a broad maximum at $2\theta \approx 16°$ that is characteristic for the amorphous structure. Samples prepared at a higher temperature by both methods show diffraction peaks increasing in intensity with the crystallization temperature. The C and A counterparts are featured by comparable X-ray spectra; this means that the molecular order is insensitive to the preparation method. Similar 2$\theta$ spectra were also recorded in the past for other samples of PLA.[14–16] According to the referenced literature, this type of X-ray spectrum results from the pseudo-orthorhombic crystalline form classified as the $\alpha$ modification of PLA.[14] The sharpest and most intense diffraction peak is at $2\theta = 16.7°$ (020 reflection). Other marked diffraction peaks are detected at $2\theta = 14.8°$ (101 reflection), $2\theta = 19.0°$ (023 reflection), and $2\theta = 22.3°$ (121 reflection). The crystallizations of both types of samples at temperatures up to about 110°C lead to comparable intensities of the main diffraction peaks. A difference is observed for samples crystallized at higher temperatures, above 110°C: the samples crystallized from the melt exhibit a $2\theta = 16.7°$ diffraction peak slightly less intense than that for the A samples. This is explained later on the basis of morphology observations.

Further information concerning the structural organization on the lamellar level in samples C and A prepared at various temperatures was provided by SAXS experiments. In Figure 2(a,b), Lorentz-corrected SAXS distributions as the dependencies of $I\mathbf{q}^2 = f(\mathbf{q})$ for samples C and A, prepared from 90 to 130°C, are shown. Here $I$ is the scattering intensity, and $\mathbf{q}$ is the scattering vector [$\mathbf{q} = (4\pi/\lambda)\sin(\theta)$, where $\theta$ is the scattering angle and $\lambda$ is the X-ray wavelength]. It can be seen from the figure that SAXS depends on the crystallization temperature. Samples prepared below 90°C (C70, C80, A70, and A80) produce a weak and diffuse scattering pattern without distinguishable maxima in the SAXS profile and, therefore, are not

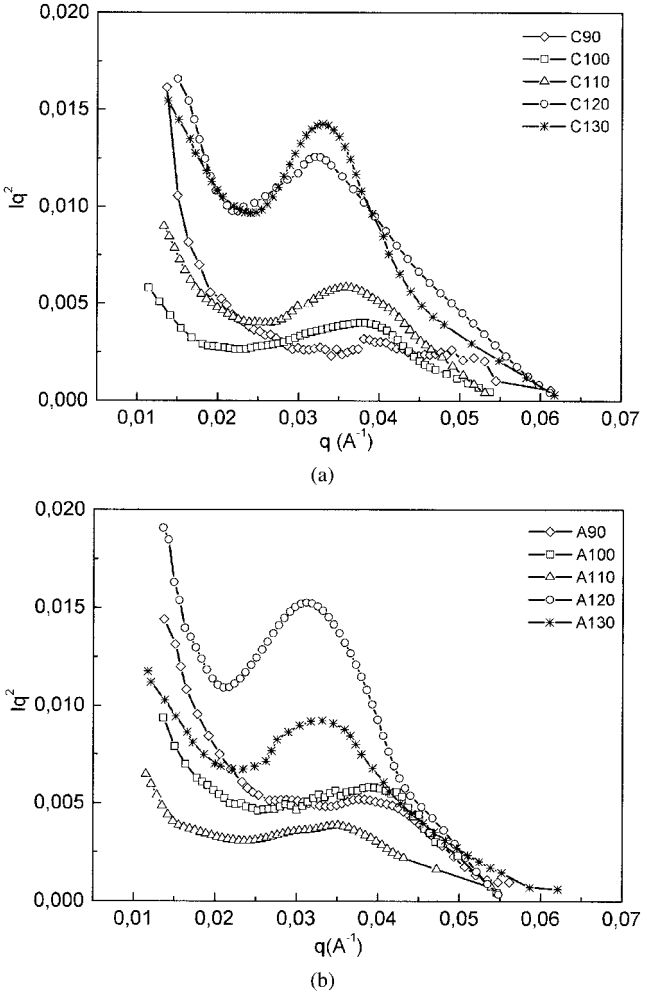


**Figure 2** Lorentz-corrected SAXS profiles for PLA samples crystallized isothermally (a) via cooling from the melt and (b) via heating from the quenched, glassy, amorphous state.

**TABLE I**
**Values of the Long Period for the Samples Crystallized Isothermally at Different Temperatures via Cooling from the Melt and via Heating from the Glassy, Amorphous State**

| Treatment temperature (°C) | Long period (Å) | |
|---|---|---|
| | Sample C | Sample A |
| 90 | 159.8 | 160.7 |
| 100 | 168.3 | 163.4 |
| 110 | 175.7 | 185.5 |
| 120 | 192.6 | 199.6 |
| 130 | 190.8 | 193.3 |

included in Figure 2. For samples prepared at a higher temperature, the maximum in the SAXS distribution appears as a result of periodicity in the arrangement of the crystalline and amorphous phases (the stacks of lamellar, amorphous regions). The periodic structure becomes better defined in the samples prepared at a higher temperature. With an increase in the crystallization temperature, the maximum intensity becomes higher and shifts toward smaller $\mathbf{q}$ (smaller angles). This shift reflects the increase in the long spacing ($L$) and, consequently, in the size of the crystallites. $L$ values for samples C and A were calculated from the Bragg relation, $L = 2\pi/\mathbf{q}_{max}$ (where $\mathbf{q}_{max}$ indicates the position of the scattering maximum), and are collected in Table I. Interestingly, the $L$ values for the C and A counterparts are nearly the same within the experimental error, and as expected, both increase with the crystallization temperature. It appears that the differentiation of the crystallization method, that is, either via cooling from the melt or via heating from the glassy, amorphous state, does not affect the long period significantly. This could indicate that the lamellar structures are not very different in the C and A counterparts. However, there is a tendency to form a slightly larger long period for A than for C (with the exception of that prepared at 100°C; see Table I). The effect can be due to some differences in the size distribution of crystallites and to the thickness of a transition layer; both result from the preparation method. Maxima in $I\mathbf{q}^2 = \mathbf{q}$ spectra are broader for A than for C prepared at the same temperature; this suggests a broader distribution of the size of the crystallites in the A samples. Furthermore, crystallization from the glassy state favors the formation of crystallites with more irregular surfaces than crystallization from the melt. Consequently, the thickness of the transition layer, contributing to the value of the long period, is expected to be larger in A than in C. Therefore, for the larger long period in A, two structural factors seem to be responsible: a broader size distribution of crystallites and a larger thickness of the transition layers than those in samples crystallized from the melt.

## Morphology

LM images at crossed polaroids for the C and A samples are shown in Figure 3. The micrographs are supplemented with the $H_v$ small-light scattering (SALS) patterns presented in Figure 4. The detailed procedure for SALS pattern analysis is described elsewhere.[13] The LM and SALS patterns for samples C and A crystallized at 70°C (and lower) are dark because of the presence of the amorphous phase only, as it was detected by X-ray methods (SALS patterns for C70 and A70 are not included in Fig. 4). The LM images of samples prepared above 70°C are brighter because of the birefringence of crystalline aggregates forming spherulites. The size of the brighter crystalline aggregates increases with the crystallization temperature; this was also confirmed by the SALS investigations. The fine spherulitic structure in samples C and A, prepared at a temperature below 120°C, produces four-leaf-clover patterns in SALS experiments. The shape of the scattered light intensity distribution of these patterns can be correlated with the size and internal perfection of the spherulites. As the spherulite size increases (for samples crystallized above 110°C), the angular intensity distribution changes; this leads to the appearance of the diffuse scattering in the central part of the scattering pattern, between the four $H_v$ leafs. With a further increase in the crystallization temperature, the central scattering increases in intensity and extends to higher angles. Finally, for samples C120, C130, A120, and A130, the SALS patterns become entirely diffusive in character, as seen in Figure 4. The dimensions of the spherulites in the samples with a fine spherulitic structure (C80, A80, C90, A90, C100, A100, C110, and A110) were calculated from the four-leaf-clover SALS patterns according to the following formula, $R = (4.09\lambda)/4\pi\sin(\theta_m/2)$,[13] where $\theta_m$ is the angle of the maximum intensity of scattering light in the azimuthal direction 45° and $\lambda$ is the wavelength of light. The dimensions were also estimated directly from the LM images for all crystalline samples. $\langle R \rangle$ values determined with both experimental techniques are given in Table II. The sizes of the spherulites in both types of samples increase with the crystallization temperature; however, they are larger in the samples crystallized via cooling from the melt than in those crystallized via heating from the glassy, amorphous state. The difference is particularly pronounced for the samples crystallized above 110°C. Spherulites in samples C120 and C130 are considerably larger than those in their counterparts A120 and A130. This follows from the much denser primary nucleation in the samples crystallized via heating from the amorphous glassy state. This can be easily explained by the formation of many embryos during the quenching of the samples of type A to the glassy state. The embryos give rise to primary nuclei of crystalli-

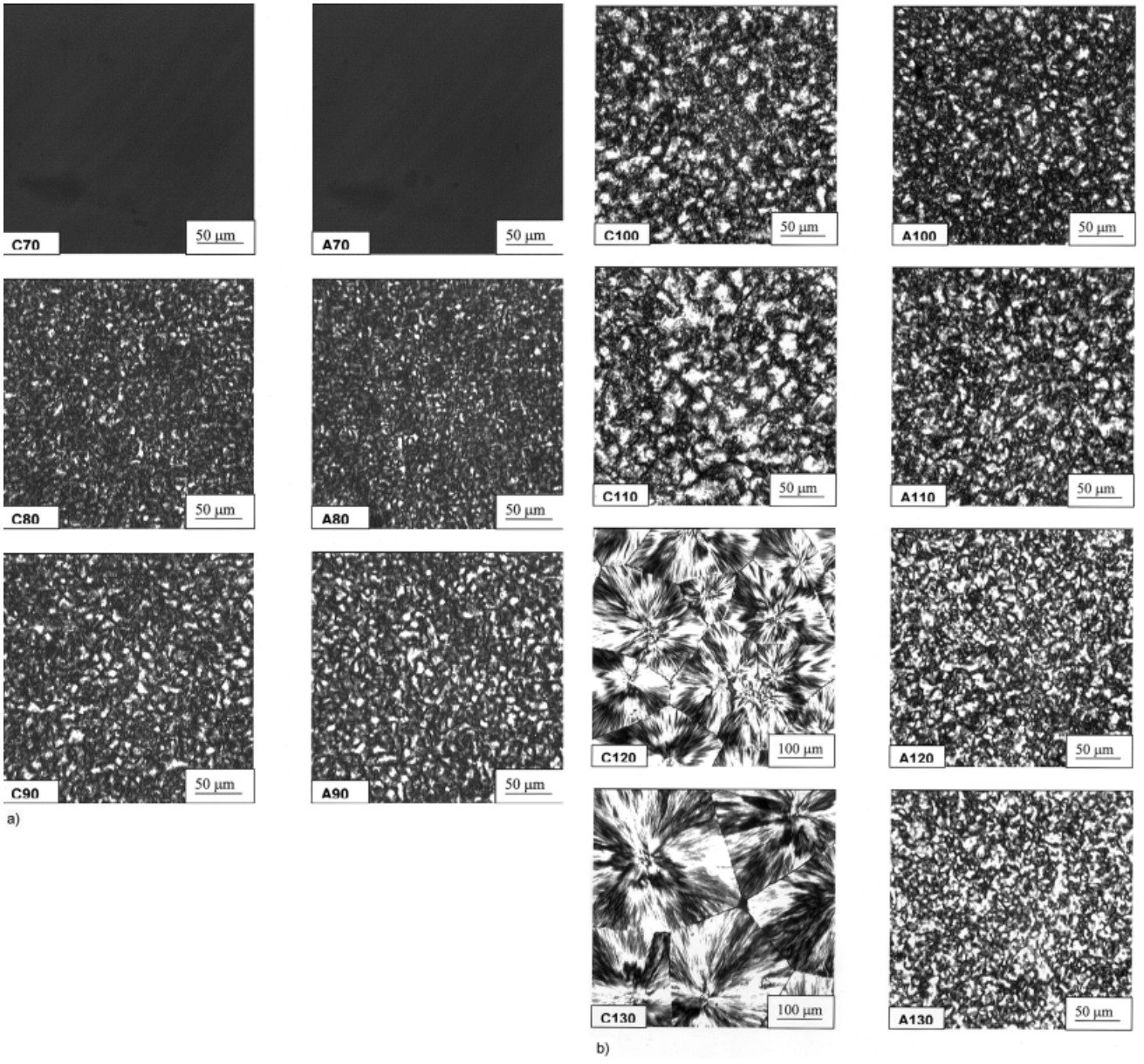


**Figure 3** Polarizing light micrographs of PLA samples crystallized isothermally via cooling from the melt (C) and via heating from the quenched, glassy, amorphous state (A) at different crystallization temperatures.

zation at a higher temperature. No such embryos were formed in the type C samples because the samples were transferred from the melt directly to the crystallization temperature.

The mean spherulite size obtained from the SALS method is larger than that determined directly from the LM images. This is because the SALS-determined size is the sixth-order momentum average characterizing the largest spherulites,[17,18] whereas in LM experiments, the first-order momentum is measured.

## Thermal behavior

Figure 5(a) presents differential scanning calorimetry (DSC) thermograms recorded during heating at a rate of 10°/min for samples C70, C80, C90, C100, C110, C120, and C130. From these thermograms, the following parameters have been determined: $T_g$, the glass-transition temperature determined from the inflection point; $T_c$ and $\Delta H_c$, the temperature of the peak position of the cold crystallization process and the heat of the cold crystallization process, respectively; $T_1$, the temperature of the onset of melting determined at the point of deviation of the thermogram from the baseline; $T_{m1}$ and $T_{m2}$, the temperatures of the melting peaks; and $\Delta H_m$, the total heat of melting. These parameters are collected in Table III. In all these thermograms, an increase in the heat flow above 60°C is seen, and it is ascribed to $T_g$ of PLA. Therefore, it is more pronounced for the samples with lower crystallinity,

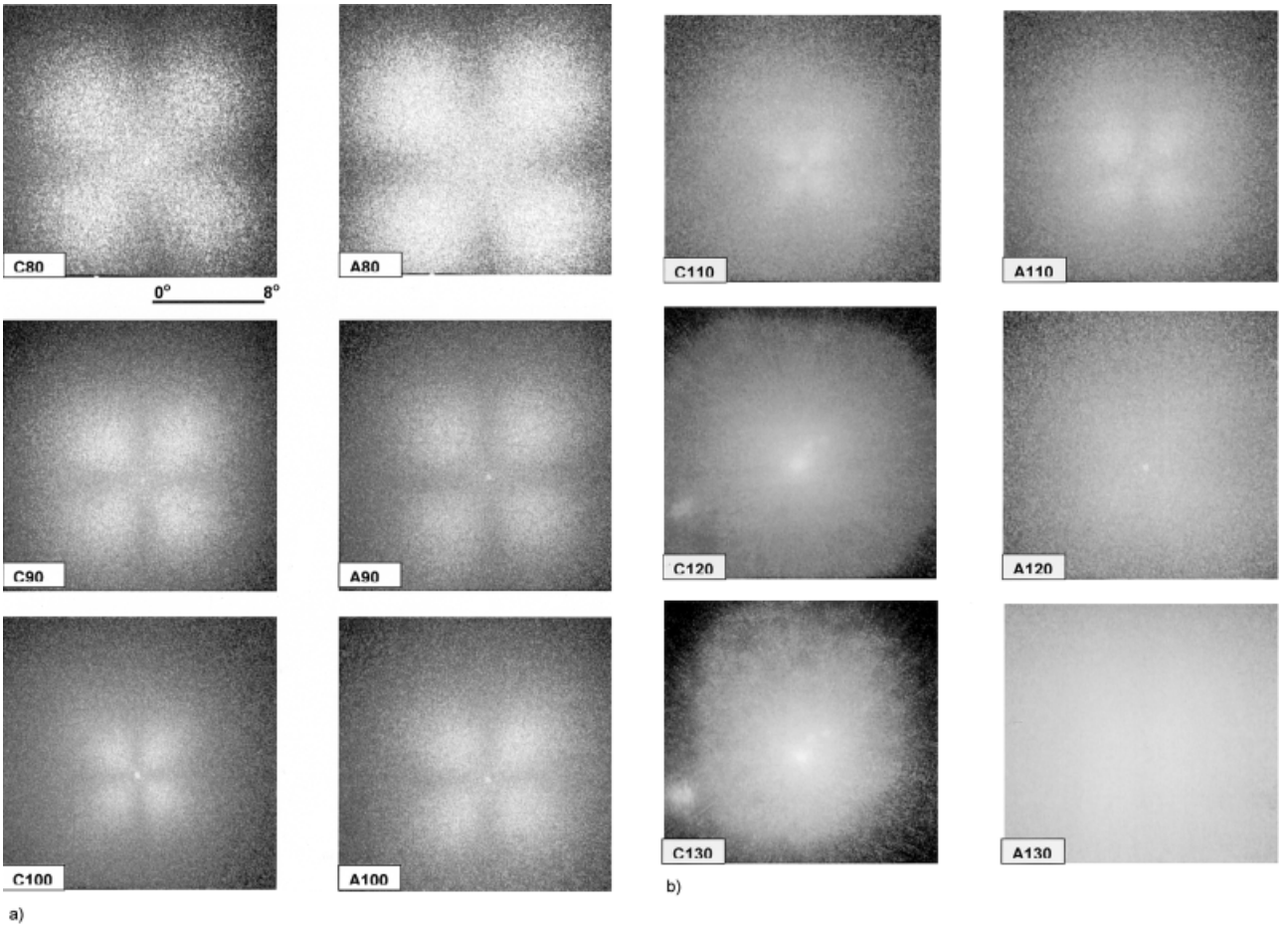


**Figure 4** SALS patterns for PLA samples crystallized isothermally (a) via cooling from the melt and (b) via heating from the quenched, glassy, amorphous state at different temperatures.

that is, those crystallized at a lower temperature. Samples C70 and C80 undergo recrystallization upon heating, which is demonstrated by a weak crystallization exothermic peak with a broad maximum in the vicinity of 130°C. The exothermic effect for samples A70 and C70 cannot be seen on curves plotted on the scale in Figure 5(a,b). For sample C70, the difference in $\Delta H_m$ and $\Delta H_c$ is insignificant (0.65 J/g; see Table III) in comparison with the heat of fusion of 100% crystalline PLA (93 J/g[19]). This indicates that the sample solidified at 70°C or lower contains an almost entirely amorphous phase. Sample C80, despite a higher degree of initial crystallinity (defined as the difference between $\Delta H_m$ and $\Delta H_c$; see Table III), exhibits a more intense crystallization exotherm than sample C70. This interesting phenomenon implies that in sample C80, during annealing at 80°C for 6 h, a number of nuclei were formed, giving rise to the formation of a fraction of the crystalline phase. These nuclei became active during the DSC scan at a temperature greater than 100°C. For samples crystallized at a temperature greater than 80°C, no cold crystallization exotherm can be observed during heating at a rate of 10°C/min. If some exothermic effect takes place, it is hidden in the low-temperature shoulder of the melting endotherm. $T_1$, determined as the point of deviation of the DSC curve from the baseline, is shown in Figure 5(a) by arrows and is

**TABLE II**
$\langle R \rangle$ Values in Samples C and A as Determined from SALS and from Polarizing light-micrographs-LMs

| | $\langle R \rangle$ ($\mu$m) | |
|---|---|---|
| Sample | SALS | LM |
| C70 | — | — |
| A70 | — | — |
| C80 | 6.8 | 2.6 |
| A80 | 5.5 | 2.6 |
| C90 | 9.9 | 4.0 |
| A90 | 7.8 | 3.5 |
| C100 | 16.4 | 7.0 |
| A100 | 10.9 | 4.6 |
| C110 | 21.5 | 8.2 |
| A110 | 13.6 | 4.8 |
| C120 | | 100.0 |
| A120 | | 3.0 |
| C130 | | 200.0 |
| A130 | | 4.0 |

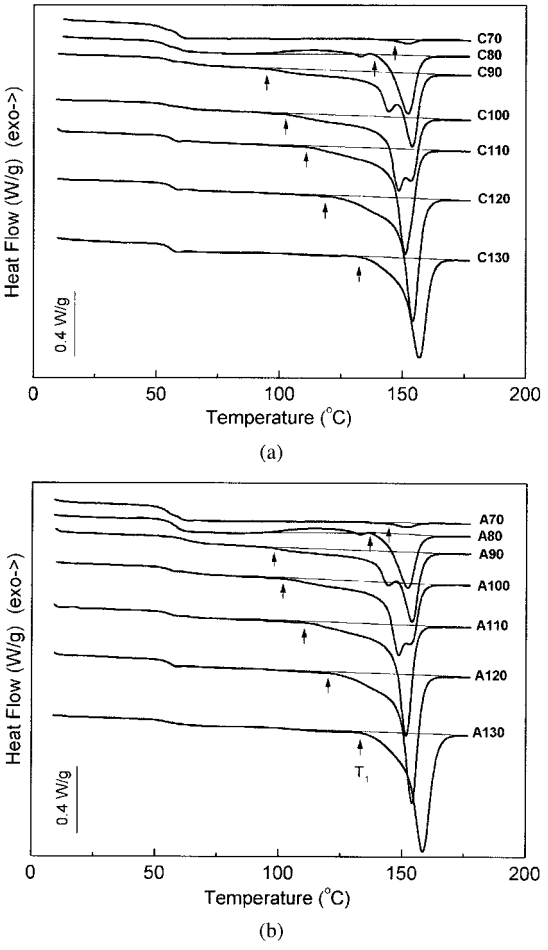


**Figure 5** DSC heating thermograms of PLA samples crystallized isothermally (a) via cooling from the melt and (b) via heating from the quenched, glassy, amorphous state at different crystallization temperatures.

listed in Table III. $T_1$ coincides well with the temperature of the sample crystallization. Apparently, the smallest and less ordered crystals formed at the crystallization temperature undergo melting at a slightly higher temperature. $\Delta H_m$ increases with the increase in the crystallization temperature (Table III). Samples C80, C90, and C100 exhibit double melting peaks with maxima at $T_{m1}$ and $T_{m2}$ (Table III). The double melting peaks reflect the melting of two populations of crystallites differing in size and internal perfection. The low-temperature melting peak shifts toward a higher temperature and increases in intensity with the increase in the crystallization temperature. Finally, it merges with the higher temperature melting peak for samples C110, C120, and C130. Consequently, the higher the crystallization temperature is, the lower the amount is of less ordered crystals. These observations indicate that the structure of the PLA samples is complex and depends strongly on the thermal history.

Figure 5(b) presents DSC thermograms of samples A70, A80, A90, A100, A110, A120, and A130. In Table IV, the calorimetric parameters are collected for these samples. The behavior of type A samples during DSC heating is strikingly similar to that of type C samples crystallized at the same temperature. This reveals that the major factor influencing the thermal properties of the investigated PLA samples is the temperature of the sample preparation (at a fixed time of the crystallization). The method of crystallization, from the melt or from the glassy, amorphous state, does not play a significant role in differentiating the thermal behavior of PLA during DSC heating.

Moreover, the value of $T_g$ determined by the DSC technique does not change significantly with the method of crystallization or with the temperature of crystallization. The values of $T_1$ and $\Delta H_m$ are comparable for samples C and A and increase with the crystallization temperature. The degree of the initial crystallinity of the samples was calculated from the difference of $\Delta H_m$ and $\Delta H_c$, with the heat of fusion assumed to be 93 J/g for 100% crystalline PLA.[19] The degree of the initial crystallinity for samples C and A is plotted in Figure 6 versus the crystallization temperature (a point for the sample solidified at room temperature, C20, is added). One can distinguish three temperature regions specified by the magnitude of the crystallinity change. In the first one, from 20 to 70°C, the initial amorphous structure is maintained. The crystallization in the temperature region from 70 to 100°C leads to a rapid increase in crystallinity. Above 100°C, the increase in crystallinity is smaller and fi-

**TABLE III**
**Calorimetric Data Derived from the Heating DSC Scan for PLA Samples Crystallized Isothermally via Cooling from the Melt at Different Temperatures**

| | | Cold crystallization | | Melting | | | |
|---|---|---|---|---|---|---|---|
| Sample | $T_g$ (°C) | $T_c$ (°C) | $\Delta H_c$ (°C) | $T_1$ (°C) | $T_{m1}$ (°C) | $T_{m2}$ (°C) | $\Delta H_m$ (°C) |
| C70 | 56.2 | 129.4 | 0.48 | 146.0 | — | 152.1 | 1.13 |
| C80 | 54.1 | 113.2 | 3.57 | 138.0 | 132.8 | 152.2 | 20.5 |
| C90 | 56.1 | — | — | 94.5 | 144.4 | 153.9 | 39.1 |
| C100 | 54.3 | — | — | 101.0 | 148.4 | 153.3 | 42.3 |
| C110 | 56.0 | — | — | 108.8 | — | 151.1 | 43.9 |
| C120 | 56.8 | — | — | 119.0 | — | 154.2 | 44.7 |
| C130 | 56.2 | — | — | 132.0 | — | 157.0 | 43.0 |

**TABLE IV**
**Calorimetric Data Derived from the Heating DSC Scan for PLA Samples Crystallized Isothermally via Heating from the Quenched, Glassy, Amorphous State at Different Temperatures**

| | | Cold crystallization | | Melting | | | |
|---|---|---|---|---|---|---|---|
| Sample | $T_g$ (°C) | $T_c$ (°C) | $\Delta H_c$ (°C) | $T_1$ (°C) | $T_{m1}$ (°C) | $T_{m2}$ (°C) | $\Delta H_m$ (°C) |
| A70 | 54.7 | 129.0 | 0.49 | 145.0 | — | 151.3 | 1.34 |
| A80 | 58.2 | 113.6 | 4.21 | 136.5 | 132.8 | 152.2 | 19.1 |
| A90 | 61.7 | — | — | 95.0 | 144.4 | 153.9 | 37.4 |
| A100 | 56.4 | — | — | 101.8 | 148.6 | 152.8 | 41.9 |
| A110 | 56.2 | — | — | 110.7 | — | 151.6 | 43.1 |
| A120 | 56.6 | — | — | 121.0 | — | 154.3 | 44.2 |
| A130 | 56.2 | — | — | 132.0 | — | 158.5 | 46.4 |

nally levels off. The dependence shown in Figure 6 illustrates the extent of structural alternations induced by thermal treatment during the processing of PLA materials of low initial crystallinity.

### Viscoelastic properties

The temperature dependencies of $E'$ determined for the samples crystallized via cooling from the melt (C type) are shown in Figure 7(a). The $E'$ curve for sample C20 is also shown. Sample C130 was susceptible to easy brittle fracture because of fragility resulting from the high crystallinity and presence of microvoids (weak places) between large and well-developed spherulites formed on account of localized volume deficiencies.[20] For this sample, no reliable viscoelastic response could be measured. The characteristic drop in the $E'$ value between 60 and 90°C due to the glass transition of PLA is seen in Figure 7(a). The decrease is more abrupt for the samples crystallized at a lower temperature (C20, C70, and C80) as a result of their low crystallinity. The increase in the $E'$ value observed for these samples above 90°C, with a maximum around 130°C, reflects the increase in the rigidity of these samples due to the recrystallization. The magnitude of this process, expressed by the $E'$ increment, is larger for sample C70 than for C20. This is in agreement with the DSC results pointing out that the presence of small crystallites and/or nuclei facilitate the recrystallization process. Samples C90 to C120 are characterized by considerably higher crystallinity (cf.

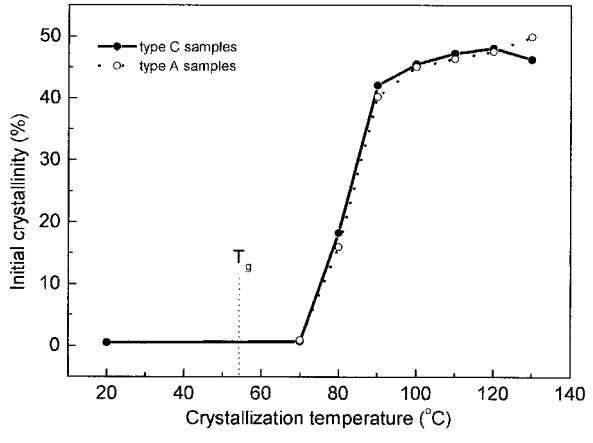


**Figure 6** Changes in the initial crystallinity versus the temperature of crystallization for the PLA samples crystallized isothermally via cooling from the melt (continuous line) and via heating from the quenched, glassy, amorphous state (dashed line).

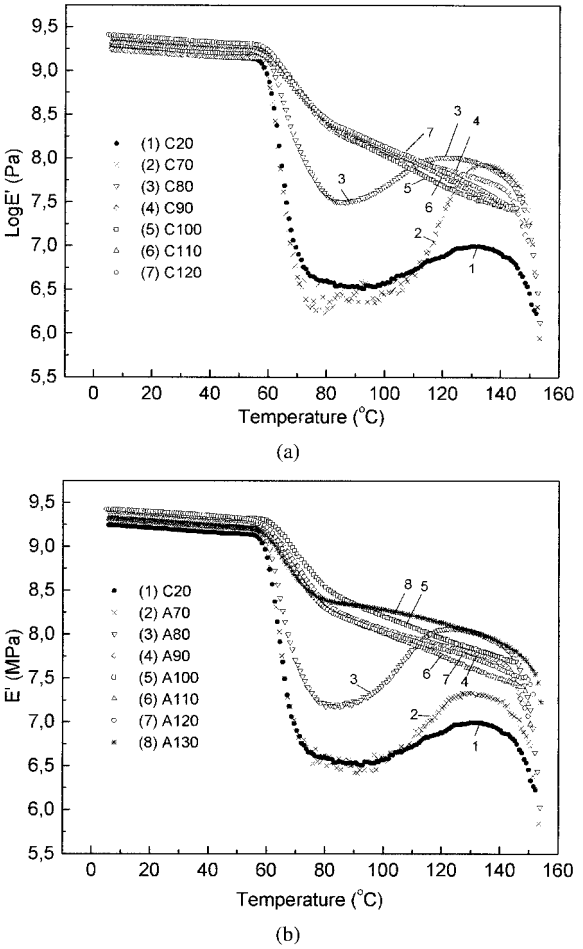


**Figure 7** $E'$ versus temperature for PLA samples crystallized isothermally (a) via cooling from the melt and (b) via heating from the quenched, glassy, amorphous state.

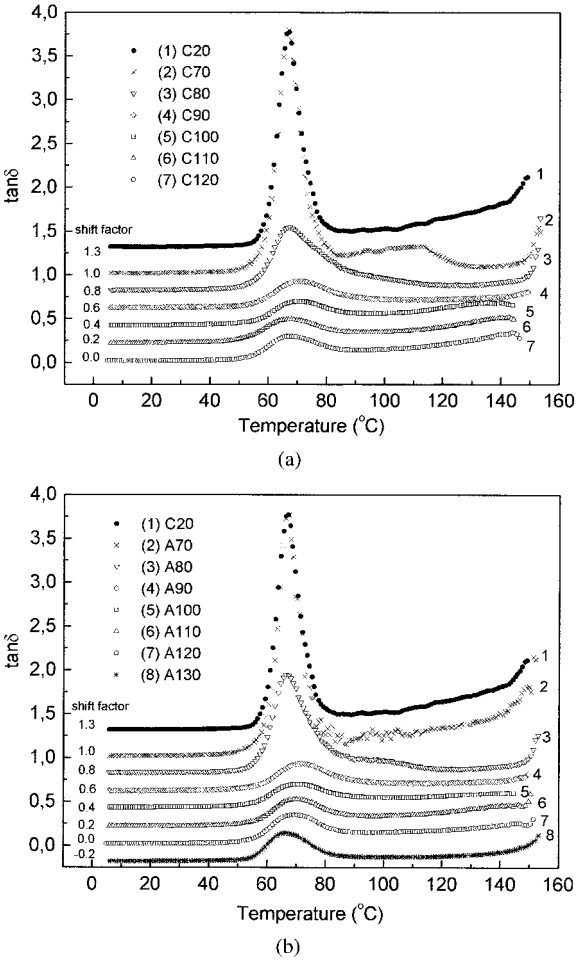


**Figure 8** Dependencies of tan δ versus temperature for the PLA samples crystallized isothermally (a) via cooling from the melt and (b) via heating from the quenched, glassy, amorphous state.

Fig. 6); therefore, in the $T_g$ region, they exhibit a moderate drop in $E'$ with increasing temperature. With a further increase above 90°C, these samples show a continuous decrease in $E'$ due to softening of the crystalline phase and a drop in the intrinsic viscosity of the amorphous phase; a premelting of smaller crystals can occur.

The temperature dependencies of $E'$ for the samples crystallized via heating from the glassy, amorphous state (type A) are presented in Figure 7(b). Their behavior closely resembles the mechanical activity for the type C counterparts. Here we were able to measure the dynamic mechanical properties of the type A sample crystallized at 130°C because this sample was less brittle because of its finer spherulitic structure. It follows then that the temperature dependence of $E'$ of PLA depends mostly on the level of crystallinity, with a minor role for the supermolecular structure (spherulite sizes).

In Figure 8(a), the mechanical loss (tan δ) of the C samples is plotted against the temperature. Analogous dependencies for the type A samples are presented in Figure 8(b). These plots clearly illustrate the tan δ changes at the glass-transition and α-relaxation regions. Around 60°C, a tan δ maximum appears (accompanied by a drop in $E'$) that is attributed to the β-relaxation process originating from the glass transition of PLA. At a higher temperature, the α-relaxation process is activated and is assigned to the relaxation phenomena connected to the presence of the crystalline phase. It is clear that the β-relaxation peak is the strongest for the samples containing the largest amount of the amorphous phase: C20, C70, and A70. The height of this peak successively decreases with the increase in the crystallinity of the polymer, and this tendency is similar for the C and A counterparts. Contrary to the DSC data, the temperature of the β-relaxation peak, corresponding to the glass-transition temperature [$T_g(\beta)$], varies for samples crystallized at different temperatures, as can be seen in Figure 8(a,b). The largest increase in $T_g(\beta)$ is observed for samples C90 and A90, which are characterized by fine spherulitic structures and comparable degrees of crystallinity. The increase in $T_g(\beta)$ is slightly smaller for the samples crystallized at higher temperatures, probably because of the reduction of the number of tie molecules and the weaker connection between the crystalline and amorphous phases. Generally, the presence of the crystalline phase increases the $T_g(\beta)$ value. This reflects the reduction of the mobility of the amorphous chains and/or their segments at the glass-transition region. In fact, the presence of the crystalline phase acts as a physical network that restricts the mobility of the surrounding amorphous phase.

The relationships between $T_g$ and the thermal history (the aging time and aging temperature) were investigated for glassy, amorphous PLA.[21] An increase in $T_g$ with an increase in the aging temperature from room temperature up to 48°C (i.e., lower than $T_g$) was found. However, the samples considered in this article were subjected to a more drastic heat treatment involving crystallization.

The mechanical losses in the α region observed for the type A and C samples crystallized at the same temperature are very similar. The tan δ behavior is, however, dependent on the initial structure of the sample: for sample A70 (and also C20), tan δ continuously increases with the temperature, whereas for sample C70, it exhibits a maximum between 80 and 120°C, and above 110°C, tan δ drops to a lower value. For the samples crystallized at a slightly higher temperature, C80 and A80, some initial increase in tan δ is also seen in the temperature region from 80 to 120°C. The structural alternations induced by annealing with increasing temperature during the DMTA measurements affect the relaxation phenomena in these samples. The samples with more stable structures, prepared between 90 and 110°C, show comparable tan δ

curves that only slightly increase with the temperature. The mechanical loss of samples C120, A120, and A130 behaves similarly; however, the intensity of tan $\delta$ peaks is even lower. From these results, it follows that the mechanical loss in the $\alpha$-relaxation region is influenced markedly by the crystallinity level. Differentiation of the supermolecular structure distinctly seen between samples C and A crystallized above 100°C (Fig. 3) does not play a substantial role in the modification of the $\alpha$-relaxation process. The only difference revealed for these samples is a slightly higher tan $\delta$ in the $\alpha$-relaxation region for the type C samples. The increase results from the higher structural heterogeneity of coarse spherulitic C samples, which develop a concentration of stresses within interspherulitic regions and generate an additional contribution to the mechanical loss.

## CONCLUSIONS

It has been shown that the molecular and supermolecular structure of the PLA investigated can be easily controlled by the selection of the temperature and method of crystallization. Two methods of isothermal crystallization have been employed, the crystallization temperature being reached either (1) via cooling from the melt or (2) via heating from the quenched, glassy state. Quenched, glassy samples of PLA crystallize as well as the samples cooled from the melt in a similar temperature range, and we have concluded that samples crystallized by the two methods at the same temperature show similar lamellar crystalline features. The crystallinity level increases with the crystallization temperature. At the same time, the evolution of the supermolecular structure into a spherulitic form occurs. A spherulitic structure is formed in both types of samples crystallized above 70°C. The size of the spherulites increases with the temperature of crystallization; however, in samples crystallized above 100°C via cooling from the melt, the spherulites are much larger than those in the samples crystallized via heating from the glassy, amorphous state. This significant effect results from the formation of many embryos during the quenching of samples of type A to the glassy state. The embryos give rise to nuclei of crystallization at a higher temperature. No such embryos are formed in type C samples because they are transferred directly from the melt to the crystallization temperature.

The thermal properties of both types of samples crystallized at the same temperature exhibit similar features with respect to the glass-transition and melting behavior.

The viscoelastic response is more sensitive to the degree of crystallinity than the supermolecular structure, even for very different spherulite sizes. Generally, the higher the crystallinity is, the lower the mechanical loss is in the glass-transition and $\alpha$-relaxation ranges. For samples crystallized above 100°C via cooling from the melt (coarse spherulitic structure), the mechanical loss in the $\alpha$-relaxation region appears to be slightly higher than that for samples crystallized at the same temperatures but via heating from the glassy, amorphous phase (fine spherulitic structure).

PLA is considered to be a polymer useful for various practical applications. Its physical properties can be modified to some extent by thermal treatment. A slow crystallization process without previous quenching, which produces a large number of additional crystallization nuclei, should be avoided in film fabrication because the coarse spherulitic structure reduces the continuity and mechanical properties of the film.

The authors gratefully acknowledge Cargill-Dow Polymers, LLC, for supplying the PLA.

## References

1. Sinclair, R. G. J Macromol Sci Pure Appl Chem 1966, 33, 585.
2. Vert, M.; Schwarch, G.; Goudane, J. J Macromol Sci Pure Appl Chem 1995, 32, 787.
3. Jamshidi, K.; Hyon, S.-H.; Ikada, Y. Polymer 1988, 29, 2229.
4. Plastics from Microbes: Microbarial Synthesis of Polymers and Polymer Precursor; Mobley, D. P., Ed.; Hanser: Munich, 1994; Chapter 4.
5. Macromolecular Biomaterials; Hastings, G. W.; Ducheyne, P., Eds.; CRC: Boca Raton, FL, 1984; Chapter 6.
6. Jacobsen, S.; Fritz, H. G. Polym Eng Sci 1996, 36, 2799.
7. Ogata, N.; Jimenez, G.; Kawai, H.; Ogihara, T. J Polym Sci Part B: Polym Phys 1997, 35, 389.
8. Pluta, M.; Galeski, A.; Alexandre, M.; Dubois, Ph. J Appl Polym Sci 2002.
9. Brochu, S.; Prud'home, R. E.; Barakat, J.; Jerome, R. Macromolecules 1995, 28, 5230.
10. Tsuji, H.; Ikada, Y. Polymer 1999, 40, 6699.
11. Chun, S. W.; Kim, S. H.; Kim, Y. H.; Kang, H. J. Polym Korea 2000, 3, 333.
12. Biela, T.; Duda, A.; Pluta, M.; Galeski, A.; Penczek, S. Presented at the 38th Macromolecular Symposium of the World Polymer Congress, IUPAC MACRO 2000, Warsaw, Poland, July 9–14, 2000.
13. Stein, R. S.; Rhodes, M. B. J Appl Phys 1960, 31, 1873.
14. DeSantis, P.; Kovacs, A. Biopolymers 1968, 6, 299.
15. Grijpma, D. W.; Zondervan, G. J.; Pennings, A. J. Polym Bull 1991, 25, 327.
16. Zong, W.; Ge, J.; Gu, Z.; Li, W.; Chen, X.; Zang, Yi.; Yang, Y. J Appl Polym Sci 1999, 74, 2546.
17. Tabar, R. J.; Wasiak, A.; Hong, S. D.; Yuasa, T.; Stein, R. S. J Polym Sci Polym Phys Ed 1981, 19, 49.
18. Tabar, R. J.; Stein, R. S.; Rose, D. E. J Polym Sci Polym Phys Ed 1985, 23, 2059.
19. Fischer, E. W.; Sterzel, H. J.; Wegner, G. Kolloid Z Z Polym 1973, 251, 980.
20. Nowacki, R.; Kolasinska, J.; Piorkowska, E. J Appl Polym Sci 2001, 79, 2439.
21. Celli, A.; Scandola, M. Polymer 1992, 33, 2699.